Identification of nonferritin mitochondrial iron deposits in a mouse model of Friedreich ataxia

Megan Whitnall[a,1], Yohan Suryo Rahmanto[a,1], Michael L.-H. Huang[a,1], Federica Saletta[a], Hiu Chuen Lok[a], Lucía Gutiérrez[b,c], Francisco J. Lázaro[d], Adam J. Fleming[c], Tim G. St. Pierre[c], Marc R. Mikhael[e], Prem Ponka[e,2], and Des R. Richardson[a,2]

[a]Department of Pathology, University of Sydney, Sydney 2006, Australia; [b]Instituto de Ciencia de Materiales de Madrid/Consejo Superior de Investigaciones Científicas, Cantoblanco, 28049 Madrid, Spain; [c]School of Physics, University of Western Australia, Perth 6009, Australia; [d]Departamento de Ciencia y Tecnología de Materiales y Fluidos, Universidad de Zaragoza, 50018 Zaragoza, Spain; and [e]Lady Davis Institute for Medical Research, McGill University, Montreal, QC, Canada H3T 1E2

Edited by Solomon H. Snyder, The Johns Hopkins University School of Medicine, Baltimore, MD, and approved October 9, 2012 (received for review September 10, 2012)

There is no effective treatment for the cardiomyopathy of the most common autosomal recessive ataxia, Friedreich ataxia (FA). This disease is due to decreased expression of the mitochondrial protein, frataxin, which leads to alterations in mitochondrial iron (Fe) metabolism. The identification of potentially toxic mitochondrial Fe deposits in FA suggests Fe plays a role in its pathogenesis. Studies using the muscle creatine kinase (MCK) conditional frataxin knockout mouse that mirrors the disease have demonstrated frataxin deletion alters cardiac Fe metabolism. Indeed, there are pronounced changes in Fe trafficking away from the cytosol to the mitochondrion, leading to a cytosolic Fe deficiency. Considering Fe deficiency can induce apoptosis and cell death, we examined the effect of dietary Fe supplementation, which led to body Fe loading and limited the cardiac hypertrophy in MCK mutants. Furthermore, this study indicates a unique effect of heart and skeletal muscle-specific frataxin deletion on systemic Fe metabolism. Namely, frataxin deletion induces a signaling mechanism to increase systemic Fe levels and Fe loading in tissues where frataxin expression is intact (i.e., liver, kidney, and spleen). Examining the mutant heart, native size-exclusion chromatography, transmission electron microscopy, Mössbauer spectroscopy, and magnetic susceptibility measurements demonstrated that in the absence of frataxin, mitochondria contained biomineral Fe aggregates, which were distinctly different from isolated mammalian ferritin molecules. These mitochondrial aggregates of Fe, phosphorus, and sulfur, probably contribute to the oxidative stress and pathology observed in the absence of frataxin.

transferrin receptor 1 | ferroportin 1 | hemojuvelin | heme oxygenase

Tissue iron (Fe) loading leads to toxicity due to the ability of Fe to generate toxic reactive oxygen species (ROS) that may be more pronounced in the highly redox-active mitochondrion (1). Mitochondrial Fe loading is associated with the pathogenesis of the severe disease, Friedreich ataxia (FA) (1). FA is caused by insufficient expression of the mitochondrial protein, frataxin (1, 2), which leads to mitochondrial Fe accumulation (1). Frataxin facilitates iron sulfur cluster (ISC) generation and heme synthesis (1–4), with its deletion leading to oxidative stress and cardiac and neuronal degeneration (1, 2, 4).

In addition to mitochondrial Fe loading, deletion of frataxin also causes cytosolic Fe deficiency (4, 5). In the heart, frataxin deletion: (*i*) increases Fe uptake via up-regulation of transferrin (Tf) receptor 1 (TfR1) and (*ii*) targets Fe to the mitochondrion causing mitochondrial Fe overload (4, 5). Concurrently, there is decreased cytosolic Fe and down-regulation of the Fe storage protein, ferritin, indicating cytosolic Fe deficiency (4, 5). Whereas mitochondrial Fe-loading appears significant in FA pathogenesis, cytosolic Fe deficiency could also play a role as it induces cell death (6). Considering this, we assessed the therapeutic effect of dietary Fe supplementation on correcting the cytosolic Fe deficiency in muscle creatine kinase (MCK) conditional frataxin knockout mice (2). These mutants lack frataxin in the heart and skeletal muscle only and exhibit classical traits of FA cardiomyopathy, including cardiac hypertrophy, ISC enzyme deficiency, and mitochondrial Fe loading from 7 wk of age (2, 4, 5).

Our results show that dietary Fe supplementation limits MCK mutant cardiac hypertrophy. Further, we report a unique effect of frataxin deletion on systemic Fe metabolism, which leads to increased systemic Fe levels. Finally, to assess the form of mitochondrial Fe loading in the mutant heart, native chromatography, transmission electron microscopy (TEM), Mössbauer spectroscopy, and alternating current (AC) magnetic susceptibility measurements were performed. These studies in a mammalian FA model uniquely show that Fe accumulating in mutant mitochondria in the heart is a biomineral aggregate distinctly different from mammalian ferritin.

Results

Fe Supplementation Delays Weight Loss and Limits Cardiac Hypertrophy. The MCK mutant heart suffers a cytosolic Fe deficiency (4, 5) and a lack of ISCs precedes the cardiomyopathy (2). Hence, the therapeutic role of dietary Fe supplementation in the restoration of these deficiencies was assessed and may lead to reconstitution of Fe in cytosolic pools. In these studies, wild-type (WT) and mutant mice were maintained on a diet of normal Fe (0.02% Fe/kg) or high Fe (2.00% Fe/kg) from 4.5 to 8.5 wk of age. These ages were chosen as no overt phenotype in mutants is present at 4.5 wk, whereas at 8.5 wk, a severe cardiomyopathy is found (2, 5). Dietary Fe supplementation led to a slight, but not significant increase in WT and mutant mouse weight, relative to those on a normal Fe diet (Fig. 1*A*). Whereas mutants begin to lose weight at 6–7 wk (2), a high Fe diet marginally ameliorated this from 7.5 wk (Fig. 1*A*).

Heart weight and the heart-to-body weight ratio are important indices of cardiac hypertrophy (2, 5). Consistent with previous studies (2, 5), mutants fed a normal Fe diet showed a significant ($P < 0.001$) increase in the heart-to-body weight ratio compared with their WT counterparts at 8.5 wk of age (Fig. 1*B*). Mutants receiving the high Fe diet also showed a significant ($P < 0.001$) increase in the heart-to-body weight ratio relative to their WT counterparts. However, the extent of cardiac enlargement was significantly less ($P < 0.001$) in mutants fed a high Fe diet relative to those fed a normal Fe diet (Fig. 1*B*). Collectively, dietary Fe

Author contributions: M.W., D.R.R., and P.P. designed research; M.W., Y.S.R., M.L.-H.H., F.S., H.C.L., L.G., F.J.L., A.J.F., T.G.S.P., and M.R.M. performed research; M.W., Y.S.R., M.L.-H.H., F.S., H.C.L., L.G., F.J.L., A.J.F., and T.G.S.P. analyzed data; and M.W., Y.S.R., M.L.-H.H., D.R.R., and P.P. wrote the paper.

The authors declare no conflict of interest.

This article is a PNAS Direct Submission.

[1]M.W., Y.S.R., and M.L.-H.H. contributed equally to this work.

[2]To whom correspondence may be addressed. E-mail: prem.ponka@mcgill.ca or d.richardson@med.usyd.edu.au.

This article contains supporting information online at www.pnas.org/lookup/suppl/doi:10.1073/pnas.1215349109/-/DCSupplemental.

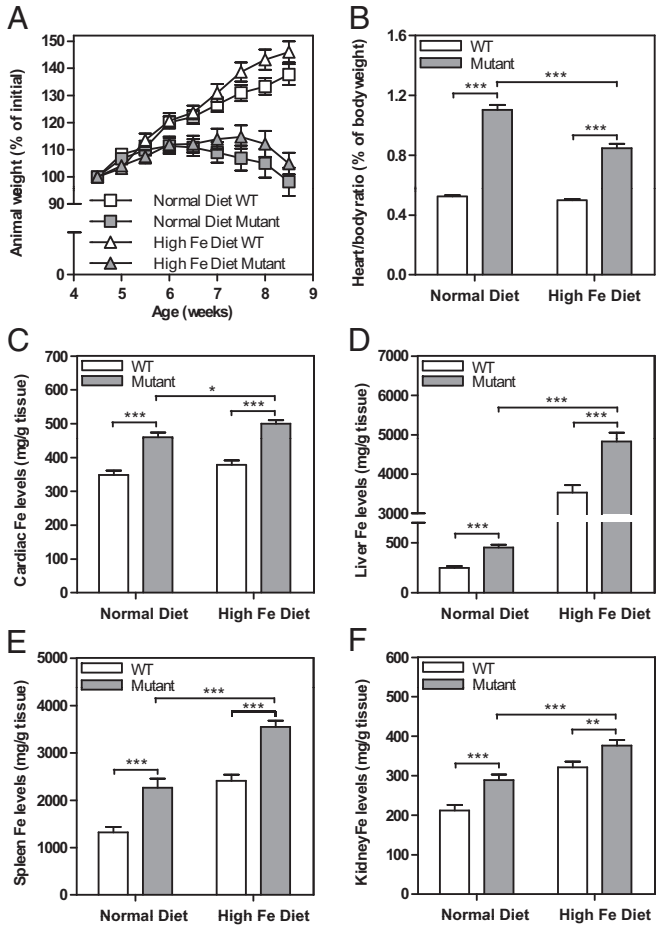

Fig. 1. Dietary Fe supplementation (*A*) does not significantly rescue weight loss in mutant mice, but (*B*) significantly limits cardiac hypertrophy. Frataxin deficiency in the mutant heart and skeletal muscle leads to Fe loading in the (*C*) heart, (*D*) liver, (*E*) spleen, and (*F*) kidney. WT and mutants were fed a normal (0.02% Fe/kg) or high (2.00% Fe/kg) Fe diet from 4.5 to 8.5 wk of age. Results in *A* and *B* are mean ± SEM (n = 30–38 mice); (*C*–*F*) are mean ± SEM (n = 24–30 mice). *$P < 0.05$; **$P < 0.01$; ***$P < 0.001$.

moderates, but does not totally rescue cardiac hypertrophy, probably as the extra Fe cannot totally replace frataxin function that is vital for ISC and heme synthesis (1–4).

Organ Fe Content. To assess the effect of dietary Fe loading, total Fe levels in the heart, liver, spleen, and kidney were measured using inductively coupled plasma atomic emission spectroscopy (ICP-AES) (Fig. 1 *C*–*F*). Cardiac Fe levels were significantly ($P < 0.001$) higher in normal and high-Fe-diet–fed mutants compared with WT at 8.5 wk of age (Fig. 1*C*). As shown previously, this increase of Fe in mutants fed a normal Fe diet is due to mitochondrial Fe accumulation (2, 5). Further, there was a slight, but significant ($P < 0.05$) increase in the cardiac Fe levels of mutants fed a high Fe diet (490.6 ± 11.4 μg/g; $n = 27$) relative to a normal Fe diet (460.0 ± 13.7 μg/g; $n = 24$; Fig. 1*C*). In addition, liver, spleen, and kidney Fe levels were significantly ($P < 0.001$) greater in WT and mutants fed a high Fe diet compared with their counterparts fed a normal Fe diet (Fig. 1 *D*–*F*). The largest increase in Fe levels in mice fed a high Fe diet was found in the liver, consistent with its role in Fe storage (1, 7). Of note, was the significant ($P < 0.001$) increase of Fe in the liver, spleen, and kidney of mutants relative to WT fed the normal diet (Fig. 1 *D*–*F*). In conclusion, frataxin deletion in the heart and skeletal muscle leads to Fe loading in the liver, kidney, and spleen.

Frataxin Knockout Disrupts the Normal Physiologic Response to Fe Loading in the Mutant Heart. Western analysis was then used to examine the effect of dietary Fe on the expression of Fe metabolism proteins in the heart and liver to further assess the systemic effect of frataxin deletion in the heart and skeletal muscle (2, 4). The high Fe diet relative to normal Fe diet did not significantly alter cardiac frataxin levels in mutant or WT mice (Fig. 2*A*). In agreement with previous studies assessing the heart (4, 5), mutants fed a normal Fe diet relative to WT mice exhibited: (*i*) TfR1 up-regulation; (*ii*) down-regulation of heavy chain ferritin (H-ferritin) and ferroportin1; and (*iii*) increased iron-regulatory protein (IRP) 2 levels (Fig. 2*A*) and RNA-binding activity (Fig. S1). The TfR1 is crucial for Tf-bound Fe uptake and is the main Fe acquisition pathway (8). As expected from IRP-iron responsive element (IRE) theory (8), following a high Fe diet, a significant ($P < 0.01$) decrease of TfR1 was observed in hearts of WT relative to these mice fed a normal Fe diet (Fig. 2*A*). In clear contrast, TfR1 was not significantly altered in the hearts of mutants fed a high relative-to-normal Fe diet (Fig. 2*A*).Uniquely, this indicated that in mutants, frataxin deficiency does not lead to the normal protective effect via the IRP-IRE mechanism to down-regulate TfR1 in response to increased Fe (8).

A significant ($P < 0.01$) increase in H-ferritin was found in WT mice fed a high versus normal Fe diet (Fig. 2*A*). Together with the decrease in TfR1 (Fig. 2*A*), and a slight, but significant increase in total heart Fe (Fig. 1*C*), these data demonstrate the high Fe diet led to increased cardiac Fe in WT mice. Surprisingly, in the hearts of mutants fed a high Fe diet, H-ferritin remained significantly ($P < 0.01$) down-regulated in comparison with WT mice on either diet. Again, this indicates frataxin deficiency abrogated the normal regulation of cardiac Fe metabolism in mutants fed a high Fe diet.

Ferroportin1 levels were not significantly ($P > 0.05$) changed in the hearts of WT mice fed a high Fe compared with normal diet, probably as its expression was already very high in mice fed a normal diet (Fig. 2*A*). However, ferroportin1 was markedly and significantly ($P < 0.001$) decreased in the hearts of mutants relative to their WT littermates fed a normal Fe diet (Fig. 2*A*). Interestingly, the low ferroportin1 levels in mutants was not affected by the high Fe diet. The level of IRP2 was almost undetectable in WT animals fed a normal or high Fe diet (Fig. 2*A*). In contrast, mutants fed a normal Fe diet showed a pronounced and significant ($P < 0.001$) increase in IRP2, but this was not significantly reduced in mutants fed a high Fe diet. Collectively, these data indicate that frataxin deletion prevents the normal regulation of Fe metabolism.

The MCK conditional frataxin knockout strategy leads to frataxin deletion in the heart and skeletal muscle only (2, 4). However, our studies showed that instead of the up-regulation of TfR1 and IRP2 and down-regulation of ferritin observed in the 8.5-wk-old mutant heart (Fig. 2*A*), an opposite effect was observed in skeletal muscle (i.e., down-regulation of TfR1 and IRP2 and up-regulation of ferritin-H relative to WT; Fig. S2). Hence, the indications of cytosolic Fe deficiency found in the mutant heart were not identified in the skeletal muscle of this animal. This suggested a difference in the role frataxin plays in Fe metabolism in the skeletal muscle and heart, which could relate to their distinct functions and metabolic requirements.

In addition to proteins posttranscriptionally controlled by IRP2 (i.e., TfR1, H-ferritin, ferroportin1) (8), we showed that ferrochelatase (Fech), mitochondrial ferritin, hemojuvelin (Hjv) and succinate dehydrogenase (SDHA) expression were significantly ($P <$ 0.001–0.01) decreased in hearts of mutants relative to WT mice fed a normal diet (Fig. 2*A*). Feeding mutant mice an Fe-loaded diet did not significantly alter their expression relative to mice fed a normal diet (Fig. 2*A*). Further, as shown before (4), and herein (Fig. 2*A*), heme oxygenase 1 (Hmox1) was increased in mutants relative to WT mice fed a normal diet. However, the Fe-loaded diet did not significantly affect this expression pattern. These studies showed that the expression of these proteins in mutants could not be significantly altered through Fe supplementation.

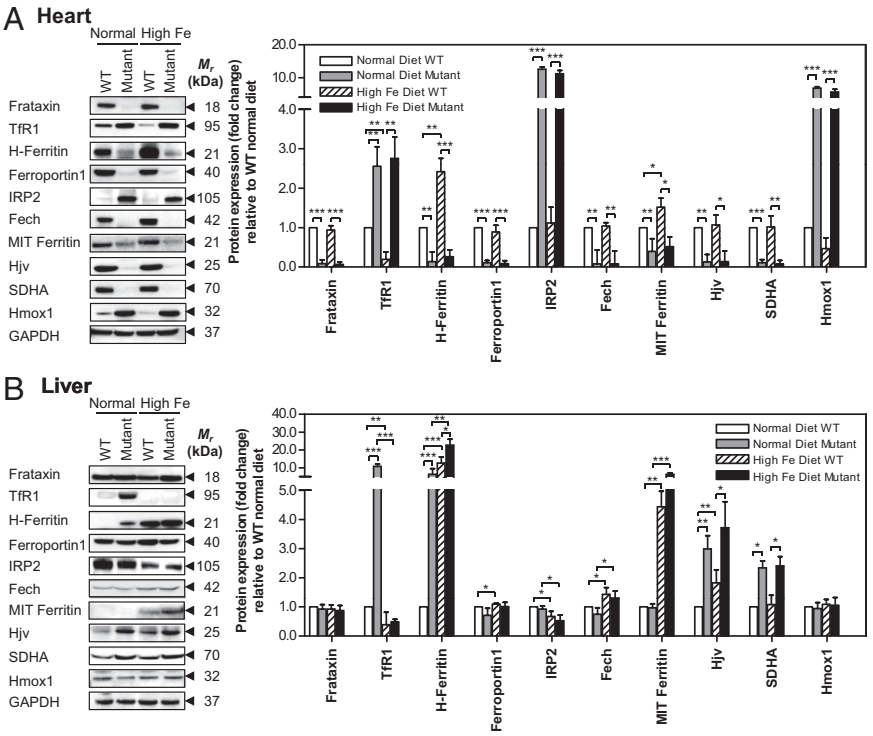

Fig. 2. Frataxin deficiency in the heart prevents the normal physiological response to dietary Fe loading in (*A*) mutant heart and (*B*) causes systemic alterations to Fe-metabolism–related proteins in the mutant liver. Westerns are typical experiments and densitometry is mean ± SD (three to five experiments). $*P < 0.05$; $**P < 0.01$; $***P < 0.001$.

IRP2–RNA-Binding Activity Is Not Reduced in Mutants' Hearts by Fe-Loading. In vivo, IRP2 regulates cellular Fe metabolism by modulating the expression of IRE-containing transcripts e.g., TfR1, ferritin, ferroportin1, etc., (1, 8, 9). In contrast, IRP1 plays a lesser role in vivo in regulating Fe metabolism (9). As shown previously (5), and again herein (Fig. S1), IRP2–RNA-binding activity was significantly ($P < 0.01$) increased in mutant hearts relative to WT mice fed a normal diet. In fact, the increased IRP2–RNA-binding activity is probably responsible for TfR1 up-regulation and down-regulation of H-ferritin and ferroportin1 in mutants (Fig. 2*A*). In contrast, IRP1–RNA-binding activity was not significantly ($P > 0.05$) altered between the mutant or WT animals, either in the presence or absence of β-mercaptoethanol (β-ME; Fig. S1), which converts IRP1 from a non–RNA-binding aconitase to an RNA-binding protein (9).

Importantly, the high IRP2–RNA-binding activity in mutants fed a normal diet was not significantly affected when they were fed a high Fe diet (Fig. S1). This finding agrees with our Western blots examining IRP2 protein levels (Fig. 2*A*) and occurs despite a significant ($P < 0.05$) increase in cardiac Fe in mutants fed a high relative to normal Fe diet (Fig. 1*C*). Considering that IRP2 is known to respond to cytosolic Fe levels (8), these results show that dietary Fe supplementation of mutants did not lead to IRP2 down-regulation. In conclusion, these data, together with the lack of response of the TfR1 and H-ferritin in mutant heart to the high Fe diet (Fig. 2*A*), indicate the regulatory response to Fe supplementation requires frataxin expression. Indeed, this Fe-dependent regulation is observed when assessing TfR1 and H-ferritin in hearts from WT mice (Fig. 2*A*).

Systemic Effects in Mutant Liver. The increase in liver, spleen, and kidney Fe in mutants fed a normal Fe diet relative to WT mice (Fig. 1 *D–F*) indicates frataxin ablation in heart and skeletal muscle not only alters cardiac Fe metabolism, but also systemic Fe processing. Considering the critical role of the liver in Fe metabolism (8), we assessed the effect of high and normal Fe diet on the expression of Fe-related proteins in this organ where frataxin expression is intact (Fig. 2*B*).

As found in the hearts of mutants fed a normal diet (Fig. 2*A*), TfR1 in the liver was also significantly ($P < 0.001$) up-regulated in mutants fed a normal diet compared with their WT counterparts (Fig. 2*B*). However, in contrast to the heart (Fig. 2*A*), TfR1 in the liver of mutants fed a high Fe diet was markedly and significantly ($P < 0.001$) down-regulated relative to mutants fed a normal diet (Fig. 2*B*). Hence, unlike the heart, the physiologic response to Fe loading in the frataxin-expressing liver was intact. Examining WT mice, a slight, but significant ($P < 0.05$) decrease in TfR1 in the liver was found comparing WTs fed a normal vs. high Fe diet (Fig. 2*B*), in agreement with IRE-IRP theory (8).

Whereas changes in the livers of WT mice fed a high Fe diet are consistent with findings following dietary Fe loading (10), the reason for the increased TfR1 in mutants fed a normal Fe diet is unclear, especially considering the significantly ($P < 0.001$) higher liver Fe in the mutant (Fig. 1*D*). However, these changes could be a consequence of frataxin deletion in the heart and skeletal muscle and may be attributed to changes in the expression of the hormone of iron metabolism, hepcidin, or other regulators of systemic Fe metabolism (1, 7, 8) (see below).

In contrast to the hearts of mice fed a normal Fe diet (Fig. 2*A*), in the liver, H-ferritin expression was significantly ($P < 0.001$) greater in mutants fed a normal Fe diet relative to WT mice (Fig. 2*B*). This finding reflects the significantly ($P < 0.001$) higher liver Fe in mutants relative to the WT mice fed a normal Fe diet (Fig. 1*D*). The extent of H-ferritin expression was greater in WT and mutant mice fed a high Fe diet relative to those fed a normal diet, in accordance with the liver's role in Fe storage (1, 7, 8).

Liver ferroportin1 and Hmox1 expression were not significantly altered in WT and mutant mice fed a normal or Fe-loaded diet (Fig. 2*B*). However, a slight, but significant ($P < 0.05$) increase in liver Fech expression was observed in WT and mutant mice fed a high Fe diet relative to their counterparts fed a normal Fe diet (Fig. 2*B*). Hjv expression in the liver was significantly ($P < 0.05$–0.01) increased in the mutant relative to the WT (Fig. 2*B*), whereas the opposite was found in the heart (Fig. 2*A*). Again, in contrast to the results obtained in the heart (Fig. 2*A*), there was no significant difference in IRP2 protein expression in the liver between WT and mutant mice fed a normal diet, despite the significantly ($P < 0.001$) greater liver Fe levels of mutants (Fig. 1*D*). However, relative to the normal Fe diet, for both WT and mutant

mice, the high Fe diet led to a significant decrease in IRP2, in agreement with its Fe-mediated degradation (8).

An intriguing finding in the mutant liver was that SDHA was significantly ($P < 0.05$) greater than for WT mice fed a normal or high Fe diet (Fig. 2*B*). This could represent systemic compensation for the metabolic defect in the heart and skeletal muscle due to frataxin deficiency. In fact, a variety of metabolic processes in the mutant heart are induced to ameliorate the energy metabolism deficiencies (11).

The results above indicate that frataxin deletion in the heart and skeletal muscle of the mutant (2) leads to marked alterations in liver Fe metabolism where frataxin expression is intact (2, 4). Indeed, the elevated TfR1 expression in the mutant (Fig. 2 *A* and *B*) occurs as part of a mechanism to increase tissue Fe.

Alteration in Serum Fe. Consistent with systemic Fe loading in 9-wk-old mutants, there was a significant ($P < 0.05$) increase in serum Fe and total Fe-binding capacity (TIBC) and a slight, but not significant increase in Tf Fe saturation relative to WT mice (Fig. S3*A*). However, no alteration was found in unbound Fe-binding capacity (UIBC). Expression of the hormone of Fe metabolism, hepcidin (7, 8), was markedly and significantly ($P < 0.001$) up-regulated in 9-wk-old mutants relative to WT mice (Fig. S3*B*). This was consistent with the high liver Fe (Fig. 1*D*) and increased Hjv (Fig. 2*B*) in this organ, which induces hepcidin expression (8). Because hepcidin decreases ferroportin1 (7, 8), it was paradoxical that relative to 9-wk-old WT mice, mutant mice fed a normal diet still expressed high duodenal ferroportin1 levels. However, the increased duodenal ferroportin1 in mutants (Fig. S3*B*) probably plays a role in the increased systemic Fe levels. Considering the markedly altered Fe metabolism in mutant, the studies described below assessed the molecular form Fe accumulating in the heart and also the liver.

Fe Accumulates in the Mutant Heart in a Mineralized Nonferritin Form. Whereas mitochondrial Fe deposits in the heart of FA patients (1) and MCK mutants (2, 5) are well documented, nothing is known about its exact molecular form in mammals. This is vital to examine, considering the potential role of mitochondrial ferritin in Fe storage in FA (1). To assess the identity of this form of Fe, size-exclusion chromatography, TEM, Mössbauer spectroscopy, and AC magnetic susceptibility were used.

Marked Alterations of ^{59}Fe Distribution in Mutant Heart. To understand how cardiac Fe is distributed within subcellular compartments, 9-wk-old WT and mutant mice were radio labeled with ^{59}Fe via tail vein injection using the Fe transport protein, Tf (^{59}Fe-Tf), and then killed 96 h later. Lysates from cytosolic and stromal mitochondrial membrane (SMM) fractions were then incubated with and without the Fe chelator, desferrioxamine (DFO; 2 mM), and separated via nondenaturing, size-exclusion chromatography. Notably, DFO was added to bind inorganic ^{59}Fe that becomes avidly bound to chromatographic separation media (12, 13). Cytosolic fractions from WT and mutant mice showed a major ^{59}Fe-containing peak in fraction 15, and two smaller peaks in fractions 20–22 and 24 (Fig. 3*A*, *i* and *ii*). The addition of DFO to WT cytosolic lysates did not lead to additional peaks (Fig. 3*A*, *i*). However, upon addition of DFO to mutant cytosolic lysates, an extra peak was found at fractions 27–28 that was not observed upon addition of DFO to WT cytosol (Fig. 3*A*, *ii*). Differences were observed in the proportion of cytosolic ^{59}Fe in these peaks between WT and mutants i.e., ^{59}Fe in fraction 15 was significantly ($P < 0.01$) greater in the WT than in mutants (Fig. 3*A*, *i* and *ii*). Purified ferritin coeluted at fraction 15, suggesting it corresponded to ferritin and these results agree with our Western data (Fig. 2*A*) and studies showing ferritin is markedly decreased in mutant hearts (4, 5). Further, total ^{59}Fe in the total cytosolic compartment was greater in WT (89,789 cpm) than in mutants (48,296 cpm), confirming mutant cytosol was Fe deficient (5).

Elution of ^{59}Fe from the SMM fraction (Fig. 3*B*) was distinctly different than the cytosolic fraction (Fig. 3*A*). Both WT and

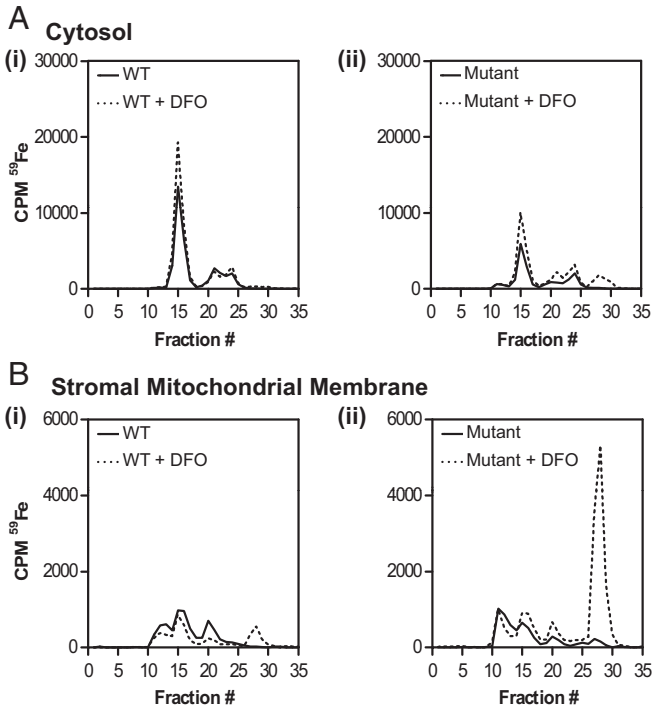

Fig. 3. Native size-exclusion chromatography of cytosolic and stromal mitochondrial membrane (SMM) fractions shows marked alterations exist in ^{59}Fe distribution in the mutant heart relative to WT heart. Total ^{59}Fe in the mutant SMM is only recovered upon treatment of the lysate with DFO. (*A*) cytosolic and (*B*) SMM fractions. Results are typical from three experiments.

mutant lysates from the SMM produced ^{59}Fe peaks in fractions 11–13, 15, 20, and 27–28 (Fig. 3*B*); although again, differences were observed in the proportion of ^{59}Fe in each fraction comparing the WT and mutant (Fig. 3*B*, *i* and *ii*). Mutant mice have markedly increased Fe within the mitochondrial compartment (2, 5). However, only after incubation of the mutant SMM fraction with DFO was sufficient ^{59}Fe eluted from the column to reflect this (Fig. 3*B*, *ii*). In the absence of DFO, only 58% of ^{59}Fe loaded onto the column was eluted from the mutant SMM, compared with 74% after incubation with DFO. Indeed, DFO induced a pronounced and significant ($P < 0.001$) increase in ^{59}Fe elution that was derived from the SMM of mutant mice in fractions 27 and 28 (Fig. 3*B*, *ii*) relative to SMM from WT's treated in the same way (Fig. 3*B*, *i*). Notably, fractions 27 and 28 correlate to those found after a solution of the DFO–^{59}Fe complex was passed through the column. Hence, most ^{59}Fe in mutant SMM became adsorbed to the chromatography media and could be eluted with DFO (Fig. 3*B*, *ii*). Similar adsorption of ^{59}Fe to chromatography media with its liberation by DFO was also seen assessing mitochondrial ^{59}Fe loading that occurs upon inhibition of heme synthesis in reticulocytes (12, 13). Collectively, marked differences exist in ^{59}Fe distribution in the cytosol and SMM of mutants compared with WT mice. Further, ^{59}Fe in mutant SMM is in a form that becomes adsorbed to chromatography media and can be solubilized by DFO.

TEM Shows Ferritin Fe Accumulation in the Mutant Liver and Nonferritin Fe in the Mutant Heart. To further assess the Fe loading in mutant hearts, unstained sections were examined using TEM (Fig. 4 *A* and *B*). Unstained sections were used to avoid the problem of heavy metal clusters that can be mistaken for ferritin and the presence of Fe was assessed by energy-dispersive X-ray analysis (Fig. S4*A*). Fig. 4 *A* and *B* show micrographs of liver and heart sections, respectively, from 9-wk-old mutants fed a normal diet. In WT heart sections, no Fe-containing particles could be observed. In the WT

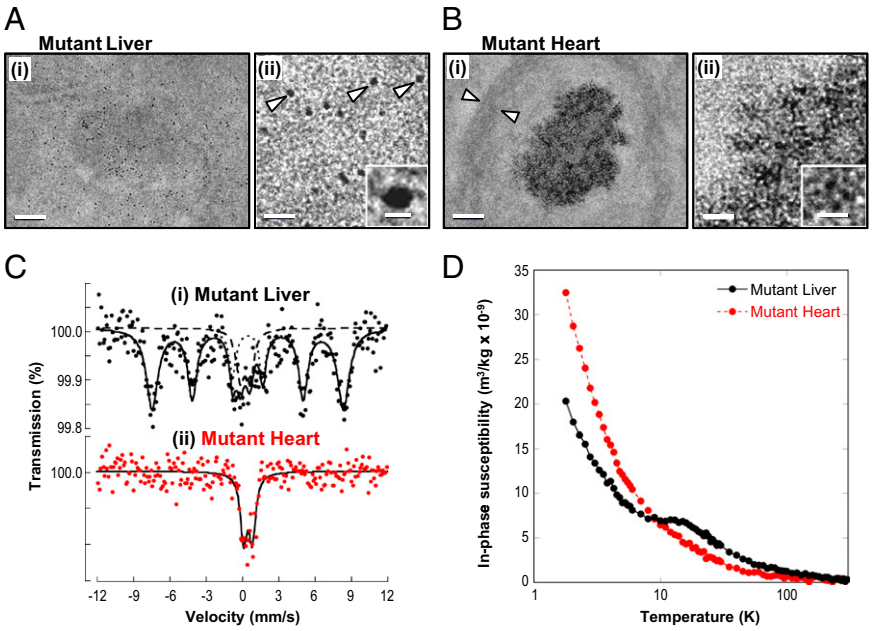

Fig. 4. In 9-wk-old mutant heart, Fe accumulates as aggregates, markedly different from mammalian ferritin found in mutant liver. TEM micrographs at (*i*) low and (*ii*) high magnification. (*A*) Mutant liver, showing isolated ferritin (arrows and *Inset*). (*B*) Mutant heart, Fe in smaller aggregates (*Inset*). Scale bars in *A* and *B*, (*i*) 100 nm and (*ii*) 25 nm; *Inset*, 6 nm. (*C*) Mössbauer spectra of 9-wk-old mutant tissues at 5 K: (*i*) liver spectrum, typical of mammalian ferritin and (*ii*) heart spectrum, Fe in a form different from mammalian ferritin. Solid lines are fits of doublets and sextets, with dotted and dashed lines representing sextet and doublet subcomponents of the fit for the liver spectrum. (*D*) At 9 wk old, Fe in mutant liver occurs as ferritin as shown by the in-phase susceptibility peak at ~13 K, whereas no such peak is found in mutant hearts. Each experimental group represents $n = 4$–10 mice.

liver, Fe-containing particles appeared similar to those in mutant liver (Fig. 4 *A*, *i* and *ii*), but appeared at a much lower frequency (Fig. S4*B*). Hence, only sections from mutant heart and liver are shown (Fig. 4 *A* and *B*), in which high Fe levels are present (Fig. 1 *C* and *D*).

Clear differences were observed in the forms of the Fe deposits in the mutant liver (Fig. 4*A*) and heart (Fig. 4*B*). In the liver of mutant mice at low magnification (Fig. 4*A*, *i*), Fe appeared in isolated, electron-dense particles. Examination of the structure of these particles at higher magnification revealed an isolated electron-dense core of 4.6 ± 1.0 nm in diameter (Fig. 4*A*, *ii*, *Inset*). This is consistent with the ultrastructure of ferritin, where the protein shell prevents contact of their Fe cores (14). In contrast, cytosolic ferritin was not evident in the mutant heart (Fig. 4*B*), because Fe is directed to the mitochondrion rather than ferritin (2, 4, 5). Unlike mutant liver, Fe in the mutant heart was found in aggregates 100–400 nm in diameter (Fig. 4*B*, *i*). These aggregates have a mitochondrial location, given the elliptical shape of the boundaries surrounding them (arrows in Fig. 4*B*, *i*). This observation is in agreement with evidence from other studies showing marked mitochondrial iron loading in mutants (2, 5). At higher magnification (Fig. 4B, *ii*), these aggregates were composed of smaller, electron-dense particles (diameter: 1.9 ± 0.6 nm; Fig. 4*B*, *ii*, *Inset*). Unlike the isolated ferritin particles in the liver that were observed at the same magnification (Fig. 4*A*, *ii*), there is no separation in the Fe-containing particles, suggesting they lack a protein shell. Energy-dispersive X-ray analysis indicated that in addition to Fe, both phosphorus and sulfur were detected in the nonferritin aggregates, but not outside them (Fig. S4*A*).

Mössbauer Spectroscopy Shows Nonferritin, Fe Loading in Mutant Heart. Mössbauer spectroscopy was then used to elucidate the speciation of Fe in the mutant heart and liver. Mössbauer spectra of mammalian ferritins exhibit magnetic hyperfine field splitting at temperatures up to several tens of kelvin (K) that result in a characteristic sextet of absorption peaks (15). Mössbauer spectra of the Fe-loaded liver of 9-wk mutants at 5 K showed a sextet and doublet signal typical of ferritin (Fig. 4*C*, *i*; sextet parameters: center shift 0.47 mm/s; quadrupole splitting 0.01 mm/s; magnetic hyperfine field splitting 48.9 T) (16). In contrast, Mössbauer spectra of the 9-wk mutant heart at 5 K (Fig. 4*C*, *ii*) exhibited no evidence of the characteristic sextet of peaks associated with mammalian ferritin (16). However, an absorption profile in the mutant heart was observed that could be fitted with a quadrupole-split doublet, which is consistent with paramagnetic high-spin Fe(III) (Fig. 4*C*, *ii*; quadrupole splitting: 0.71 mm/s; center shift relative to Fe: 0.48 mm/s with line widths of 0.66 mm/s). Thus, in mutant 9-wk-old hearts, Mössbauer spectra showed an Fe accumulation clearly different from mammalian ferritin, whereas in the liver, the Fe accumulation was typical ferritin, in good agreement with the TEM (Fig. 4 *A* and *B*).

AC Magnetic Susceptibility Shows Fe in Mutant Heart Is Not Ferritin. The magnetic properties of tissues can be characterized by AC magnetic susceptibility to assess the molecular forms of Fe present (17). As 4-wk-old mutants show no mitochondrial Fe loading, whereas mutants 9 wk old show marked mitochondrial Fe deposition (2, 5), these were compared. From the in-phase component of the AC magnetic susceptibility data (Fig. S5*A*), the structural organization of Fe within the heart can be assessed by the effective magnetic moment (μ_{eff}) (17). At 4 wk of age, no significant difference exists between the μ_{eff} of WT (2.87 ± 0.22 μ_B; $n = 3$) and mutant (2.70 ± 0.21 μ_B; $n = 3$) mice. However, at 9 wk, the μ_{eff} becomes significantly ($P < 0.05$) lower in mutants (2.17 ± 0.02 μ_B) compared with WT (2.64 ± 0.16 μ_B) (Fig. S5*A*). Hence, Fe in 9-wk-old mutant heart is different from the 4-wk mutant as well as the WT mice. Moreover, such Fe is not consistent with mammalian ferritin whose μ_{eff} is ~3.4 μ_B (17). Further, the in-phase magnetic susceptibility maximum at ~13 K in mutant liver (Fig. 4*D*) and out-of-phase maximum at ~10 K (Fig. S5*B*) are strong indicators of ferritin Fe (17). None of these features appear for mutant heart (Fig. 4*D* and Fig. S5*B*), indicating the Fe is not ferritin.

Discussion

In the mutant heart, cytosolic Fe deficiency in the presence of mitochondrial Fe loading (4, 5) provides two targets for therapeutic intervention. Indeed, the MCK mutant cardiomyopathy can be ameliorated by dietary Fe supplementation (Fig. 1*B*) and also by the targeted removal of mitochondrial Fe using chelators (5). Considering compartmental dysregulation, exogenous Fe from Fe supplementation may worsen the pathology if it is not targeted to the appropriate molecular machinery. Hence, a delicate balance using combined therapies that replenish the Fe-deficient cytosol and chelate mitochondrial Fe could be optimal.

Our work also shows that frataxin deletion in the heart and skeletal muscle leads to increased systemic Fe levels. Considering systemic controls of Fe metabolism, it is known that Hjv activates

liver hepcidin expression (8) and we showed that Hjv up-regulation occurred in the mutant liver (Fig. 2*B*), together with increased liver hepcidin levels (Fig. S3*B*). Hepcidin is known to inhibit intestinal Fe uptake by down-regulating ferroportin1 (7, 8). However, paradoxically, ferroportin1 remained high in the mutant duodenum relative to WT mice (Fig. S3*B*). The high duodenal ferroportin1 levels could explain the increased systemic Fe levels and higher serum Fe and TIBC of mutants. Relevant to these results, a study using intestinal H-ferritin knockout mice similarly showed that high hepcidin does not impair ferroportin1 levels or duodenal Fe uptake, indicating other controls, apart from hepcidin, regulate Fe absorption (18). Thus, frataxin deletion in the heart and skeletal muscle disrupts the normal control mechanisms, resulting in systemic Fe overload.

Relevant to the cardiomyopathy, systemic alterations in Fe metabolism and cytosolic Fe deficiency in the MCK mutant hearts, it is notable that previous studies assessing a mouse knockout model of copper transporter 1 show a severe cardiomyopathy, systemic alterations in copper metabolism, and cardiac copper deficiency (19). These mice exhibit elevated serum copper and increased expression of proteins involved in intestinal and liver copper acquisition and mobilization, respectively. Hence, systemic regulation of copper metabolism was observed where heart copper status led to signaling to copper storage organs (19). These findings mirror our data in MCK mutants, where up-regulation of Fe acquisition mechanisms in the duodenum and liver were observed, together with increased serum Fe, which could act as a response to correct the cardiac Fe deficiency. Hence, potential cross-organ communication may occur between the heart and organs involved in both Fe and copper acquisition and storage.

Using TEM, Mössbauer spectra and AC magnetic susceptibility, we show that cardiac Fe in mutants accumulates as nonferritin aggregates (Fig. 4 *B–D*). This observation is in contrast to mutant liver where Fe loading was shown by TEM and Mössbauer spectrometry to occur in ferritin (Fig. 4 *A*, *ii* and *C*). These findings were in agreement with Western analysis in the mutant heart, where ferritin levels were reduced (Fig. 2*A*), whereas in the mutant liver there was a marked increase in ferritin relative to WT liver (Fig. 2*B*). Interestingly, energy-dispersive X-ray spectra indicate phosphorus and sulfur in the mitochondrial nonferritin Fe aggregates. This is of interest, as previous studies showed that the intramitochondrial Fe from different origins (e.g., yeast) is based on Fe phosphates (3, 20, 21). Further, Mössbauer spectra of the mutant heart at 5 K are inconsistent with mammalian ferritin, but similar to noncrystalline, Fe phosphate minerals (3, 15). The significance of these data are crucial, as unlike ferritin, which has a protective protein shell that leads to isolated molecules in TEM, these cardiac Fe accumulations in mutants appear as coalesced aggregates, which are potentially without a protein shell (Fig. 4*B*). Thus, in the redox-active mitochondrion, such Fe without a protein coat may be an "explosive" source of ROS and would explain why antioxidants and chelators are protective in FA (5, 22).

In conclusion, dietary Fe supplementation limits cardiac hypertrophy in MCK mutants. Our results further indicate that frataxin deletion not only affects Fe metabolism of the targeted organ in the MCK mutants (e.g., heart), but also markedly influences systemic Fe metabolism. Indeed, systemic signaling in mutants increases Fe levels in tissues where frataxin expression is intact. Importantly, mitochondrial Fe accumulation in the heart due to loss of frataxin occurs as nonferritin mineral aggregates.

Materials and Methods

Animals. Mutants homozygous for deletion of *Frda* exon 4 and WT mice (2) were used under an approved University of Sydney Animal Ethics Committee protocol. Mice were fed a normal (0.02% Fe/kg) or high (2.00% Fe/kg) Fe diet (Specialty Feeds) and tissue Fe stores measured by ICP-AES (5). Blood was collected via cardiac puncture and hematological indices were assayed (6).

Western Analysis and IRP–RNA Binding. Western analysis was performed (5) using antibodies against frataxin (US Biologicals), TfR1 (Invitrogen), ferroportin1 (D. Haile, University of Texas, San Antonio, TX), GAPDH and SDHA (Santa Cruz), Fech (H. Dailey, University of Georgia, Athens, GA), H- and mitochondrial ferritin (S. Levi, San Raffaele Institute, Milan, Italy), Hmox1 (Stressgen), Hjv (S. Parkkila, University of Tampere, Tampere, Finland), IRP2 (Novus Biologicals), and hepcidin (Abcam). IRP–RNA-binding activity was performed via gel-retardation analysis (5).

See *SI Materials and Methods* for details of size-exclusion chromatography, TEM, Mössbauer spectroscopy, and AC magnetic susceptibility measurements.

ACKNOWLEDGMENTS. We thank H. Puccio and M. Koenig for MCK mice. This work was supported by the National Health and Medical Research Council, the Muscular Dystrophy Association, and the Canadian Institutes of Health Research.

1. Napier I, Ponka P, Richardson DR (2005) Iron trafficking in the mitochondrion: Novel pathways revealed by disease. *Blood* 105(5):1867–1874.
2. Puccio H, et al. (2001) Mouse models for Friedreich ataxia exhibit cardiomyopathy, sensory nerve defect and Fe-S enzyme deficiency followed by intramitochondrial iron deposits. *Nat Genet* 27(2):181–186.
3. Lesuisse E, et al. (2003) Iron use for haeme synthesis is under control of the yeast frataxin homologue (Yfh1). *Hum Mol Genet* 12(8):879–889.
4. Huang ML, et al. (2009) Elucidation of the mechanism of mitochondrial iron loading in Friedreich's ataxia by analysis of a mouse mutant. *Proc Natl Acad Sci USA* 106(38): 16381–16386.
5. Whitnall M, et al. (2008) The MCK mouse heart model of Friedreich's ataxia: Alterations in iron-regulated proteins and cardiac hypertrophy are limited by iron chelation. *Proc Natl Acad Sci USA* 105(28):9757–9762.
6. Yu Y, Suryo Rahmanto Y, Richardson DR (2012) Bp44mT: An orally active iron chelator of the thiosemicarbazone class with potent anti-tumour efficacy. *Br J Pharmacol* 165(1):148–166.
7. Richardson DR, et al. (2010) Mitochondrial iron trafficking and the integration of iron metabolism between the mitochondrion and cytosol. *Proc Natl Acad Sci USA* 107(24): 10775–10782.
8. Hentze MW, Muckenthaler MU, Galy B, Camaschella C (2010) Two to tango: Regulation of Mammalian iron metabolism. *Cell* 142(1):24–38.
9. Meyron-Holtz EG, et al. (2004) Genetic ablations of iron regulatory proteins 1 and 2 reveal why iron regulatory protein 2 dominates iron homeostasis. *EMBO J* 23(2): 386–395.
10. Ward PP, Mendoza-Meneses M, Cunningham GA, Conneely OM (2003) Iron status in mice carrying a targeted disruption of lactoferrin. *Mol Cell Biol* 23(1):178–185.
11. Sutak R, et al. (2008) Proteomic analysis of hearts from frataxin knockout mice: Marked rearrangement of energy metabolism, a response to cellular stress and altered expression of proteins involved in cell structure, motility and metabolism. *Proteomics* 8(8):1731–1741.
12. Richardson DR, Ponka P, Vyoral D (1996) Distribution of iron in reticulocytes after inhibition of heme synthesis with succinylacetone: Examination of the intermediates involved in iron metabolism. *Blood* 87(8):3477–3488.
13. Ponka P, Wilczynska A, Schulman HM (1982) Iron utilization in rabbit reticulocytes. A study using succinylacetone as an inhibitor or heme synthesis. *Biochim Biophys Acta* 720(1):96–105.
14. Iancu TC (1992) Ferritin and hemosiderin in pathological tissues. *Electron Microsc Rev* 5(2):209–229.
15. St Pierre TG, Webb J, Mann S (1989) Ferritin and hemosiderin: Structural and magnetic studies of the iron core. *Biomineralization: Chemical and Biochemical Perspectives*, eds Mann S, Webb J, Williams RJP (VCH, Weinheim, Germany), pp 295–344.
16. St Pierre TG, Chua-anusorn W, Webb J, Macey D, Pootrakul P (1998) The form of iron oxide deposits in thalassemic tissues varies between different groups of patients: A comparison between Thai beta-thalassemia/hemoglobin E patients and Australian beta-thalassemia patients. *Biochim Biophys Acta* 1407(1):51–60.
17. Gutiérrez L, Vujić Spasić M, Muckenthaler MU, Lázaro FJ (2012) Quantitative magnetic analysis reveals ferritin-like iron as the most predominant iron-containing species in the murine Hfe-haemochromatosis. *Biochim Biophys Acta* 1822(7):1147–1153.
18. Vanoaica L, Darshan D, Richman L, Schümann K, Kühn LC (2010) Intestinal ferritin H is required for an accurate control of iron absorption. *Cell Metab* 12(3):273–282.
19. Kim BE, et al. (2010) Cardiac copper deficiency activates a systemic signaling mechanism that communicates with the copper acquisition and storage organs. *Cell Metab* 11(5):353–363.
20. Grasso JA, Myers TJ, Hines JD, Sullivan AL (1980) Energy-dispersive X-ray analysis of the mitochondria of sideroblastic anaemia. *Br J Haematol* 46(1):57–72.
21. Seguin A, et al. (2011) Co-precipitation of phosphate and iron limits mitochondrial phosphate availability in Saccharomyces cerevisiae lacking the yeast frataxin homologue (YFH1). *J Biol Chem* 286(8):6071–6079.
22. Rustin P, et al. (1999) Effect of idebenone on cardiomyopathy in Friedreich's ataxia: A preliminary study. *Lancet* 354(9177):477–479.